GRID DIAGRAMS AND LEGENDRIAN LENS SPACE LINKS

Kenneth L. Baker and J. Elisenda Grigsby

Grid diagrams encode useful geometric information about knots in S^3. In particular, they can be used to combinatorially define the knot Floer homology of a knot $K \subset S^3$, and they have a straightforward connection to Legendrian representatives of $K \subset (S^3, \xi_{st})$, where ξ_{st} is the standard, tight contact structure. The definition of a grid diagram was extended, by Hedden and the authors, to include a description for links in all lens spaces, resulting in a combinatorial description of the knot Floer homology of a knot $K \subset L(p, q)$ for all $p \neq 0$. In the present article, we explore the connection between lens space grid diagrams and the contact topology of a lens space. Our hope is that an understanding of grid diagrams from this point of view will lead to new approaches to the Berge conjecture, which claims to classify all knots in S^3 upon which surgery yields a lens space.

1. Introduction

A grid diagram provides a simple combinatorial means of encoding the data of a link in S^3, as in Figure 1. Although grid diagrams first made an appearance in the late 19th century [Bru98], they have enjoyed an abundance of recent attention, due primarily to their connection to contact topology [Lyo80, Cro95, Dyn06, Mat06, OST06] and combinatorial Heegaard Floer homology [MOS06, MOST06].

The definition was extended in [BGH08] to provide a means of encoding the data of all lens space links via grid diagrams, leading to a combinatorial description of the knot Floer homology of a lens space knot. Figure 2 illustrates the notion of a lens space grid diagram; we delay its precise definition until Section 4.

In the present article, we explore the connection between the contact geometry of a lens space and grid diagrams for lens space links.
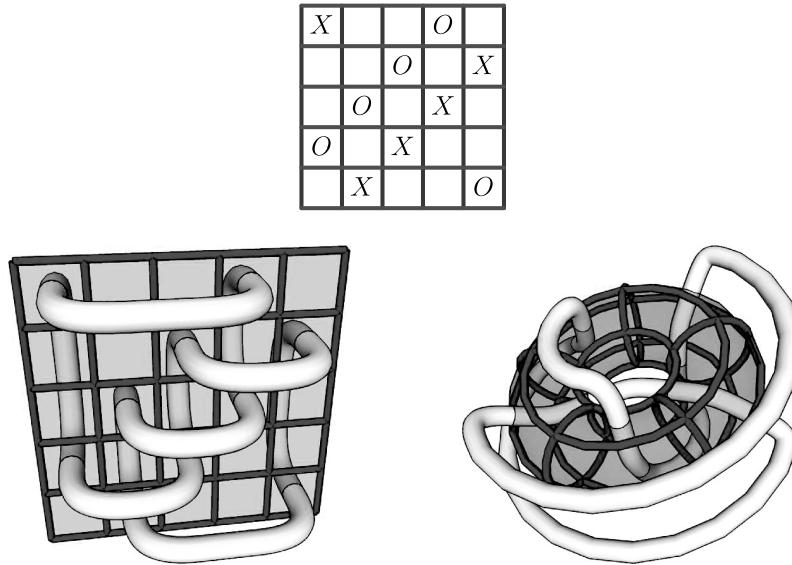
Figure 1. An S^3 grid diagram for a trefoil, along with two views of the knot it represents.

Theorem 4.4. *Associated to a grid diagram for a link K in the lens space $L(p,q)$ is a unique Legendrian representative of $m(K)$ with respect to $(-L(p,q), \xi_{UT})$.*

Here, $m(K)$ denotes the topological mirror of K and ξ_{UT} is a canonical co-oriented contact structure on $-L(p,q)$. See Section 2 for a detailed discussion of notation and orientation conventions.

Our approach is similar in spirit to that taken by Matsuda and Menasco [**MM07**]. In a very natural geometric fashion, a grid diagram describing a lens space link corresponds to a Legendrian representative of the link with respect to a canonical co-oriented tight contact structure on the lens space. A contact structure ξ on a 3-manifold M is a smooth, nowhere integrable 2-plane field. A link in the contact manifold (M, ξ) is *Legendrian* if it is everywhere tangent to ξ and *transverse* if it is everywhere transverse to ξ. A contact structure ξ is said to be *tight* if the linking number of any trivial Legendrian knot with its contact push-off is negative (equivalently, (M, ξ) contains no overtwisted disks). Furthermore, a tight contact structure ξ on a 3-manifold M is *universally tight* if the lift of ξ to the universal cover of M is also tight.

By Honda's classification [**Hon00**], each lens space $L(p,q)$ has two distinct (positive, co-oriented) universally tight contact structures when $0 < q < p-1$ and just one when $q = p-1$. Given one universally tight contact structure on

$L(p,q)$, the other is obtained by flipping its co-orientation. When $q = p - 1$, these two are isotopic.

Suppressing the specific lens space from the notation, we will denote a particular co-oriented universally tight contact structure on $L(p,q)$ by ξ_{UT}. We explicitly construct ξ_{UT} in Section 3.1.

We use *toroidal fronts* to mediate between grid diagrams and Legendrian lens space links. Just as planar fronts uniquely specify Legendrian links in $(\mathbb{R}^3, \xi_{\mathrm{st}})$ via projection to the xz-plane, toroidal fronts uniquely specify Legendrian links in $(L(p,q), \xi_{\mathrm{UT}})$ via projection to a standard Heegaard torus. After defining toroidal fronts and their correspondence with Legendrian lens space links in Section 3.2, we detail the relationship between toroidal fronts and grid diagrams in Sections 4 and 5.

1.1. Motivation. One motivation for developing the connection between grid diagrams and Legendrian lens space links (and their toroidal fronts) is to provide the foundation for a systematic study of Legendrian links in a collection of contact manifolds other than (S^3, ξ_{st}). Furthermore, certain elements in the knot Floer homology chain complex of (the mirror of) a lens space knot associated to a grid diagram should yield powerful invariants of the corresponding Legendrian or transverse representatives of the knot. In particular, one ought to be able to use such invariants to detect transversely non-simple knots in lens spaces, as Ng, Ozsváth, and Thurston did for knots in S^3 [**NOT07**].

Moreover, this work reveals an inlet for the use of contact structures in studying a fundamental question about the interconnectedness of 3-manifolds through Dehn surgery on knots. Lens spaces are precisely the manifolds that may be obtained by Dehn surgery on the unknot in S^3. The resolutions of The Knot Complement Problem [**GL89**] and Property R [**Gab87**] show that the unknot is the only knot in S^3 on which a non-trivial Dehn surgery may produce the lens spaces S^3 and $S^1 \times S^2$, respectively. For many other lens spaces, this is not the case. Indeed, all torus knots admit lens space surgeries [**Mos71**], as do certain cables of torus knots (the only satellite knots admitting lens space surgeries) [**BL89**] and many hyperbolic knots [**BR77**, **FS80**, **Ber**]. The Berge Conjecture proposes a classification of all knots in S^3 and their Dehn surgeries that yield lens spaces. Originally stated in terms of a homotopy condition for a knot embedded on the surface of a genus 2 Heegaard surface in S^3, the Berge Conjecture is most succinctly stated as follows:

Berge Conjecture ([**Ber**]). *If a knot K in a lens space $L(p,q)$, with $p \notin \{0, 1\}$, admits an S^3 Dehn surgery, then it has grid number 1.*

The *grid number*, GN, of a link is the minimum grid number over all grid diagrams representing the link. See Definition 4.1 for the definition of the grid number of a grid diagram, as well as Figure 2, which illustrates a grid

number 5 grid diagram for the trefoil in S^3. In light of the above, one might hope for an upper bound on GN for knots admitting S^3 surgeries.

For links in S^3, Matsuda [**Mat06**] proves

$$\mathrm{GN}(K) \geq -\overline{\mathrm{tb}}(K) - \overline{\mathrm{tb}}(m(K)).$$

Here, tb denotes the classical Thurston–Bennequin number associated to a Legendrian link in (S^3, ξ_{st}), and $\overline{\mathrm{tb}}(K)$ denotes the maximal Thurston–Bennequin number over all Legendrian representatives of K.

Although this provides a lower bound on grid number, Ng speculates, in [**Ng06**], that this bound may be sharp. A proof of this would imply that $\overline{\mathrm{tb}}(K)$ and $\overline{\mathrm{tb}}(m(K))$ determine $\mathrm{GN}(K)$, and thus an upper bound on the maximal Thurston–Bennequin numbers of a link and its mirror would produce an upper bound on the grid number.

For links in lens spaces, we prove an analog of Matsuda's bound in Section 6.

Corollary 6.10.
$$\mathrm{GN}(K) \geq -\overline{\mathrm{tb}}(K) - \overline{\mathrm{tb}}(m(K))$$
for each link $K \subset L(p, q)$.

This requires an extension of the definition of $\mathrm{tb}(K)$ to all Legendrian links in contact rational homology spheres, provided in Definition 6.6. See [**Özt05**] for a related extension.

If Matsuda's bound is sharp for lens space links, one can bound from above the grid number of a knot admitting an S^3 surgery by finding upper bounds for the Legendrian contact invariants $\overline{\mathrm{tb}}(K)$ and $\overline{\mathrm{tb}}(m(K))$. The hope is that suitably understanding Legendrian representatives of knots in $L(p, q)$ with S^3 surgeries will shed light on the Berge Conjecture.

2. Notation and orientation conventions

Throughout the paper, $L(p, q)$ will denote the result of $-\frac{p}{q}$ surgery on the unknot, where p and q are coprime integers such that $0 \leq |q| < p$. We view S^3 as the lens space $L(1, 0)$ and will not consider $S^1 \times S^2 = L(0, 1)$.

Let G_K be a grid diagram representing a link $K \subset L(p, q')$. Then G_K will naturally yield a Legendrian representative, which we will denote $\mathcal{L}_K$, of the topological mirror of K, $m(K) \subset (L(p, q), \xi_{\mathrm{UT}})$. Here, q satisfies $qq' \equiv -1$ mod p. Note that, by the classification of lens spaces up to orientation-preserving diffeomorphism, $L(p, q) \cong -L(p, q')$. We describe ξ_{UT} as the kernel of a globally defined 1-form in the next section.

The correspondence between a grid diagram (or, more generally, a Heegaard diagram) compatible with a knot, K, and a Legendrian representative of $m(K)$, although odd, is by now standard in the literature. See, e.g., [**OST06**], where a grid diagram for $K \subset S^3$ is associated to a Legendrian

representative of K with respect to ξ_{st} on S^3 with the opposite orientation (i.e., a Legendrian representative of the mirror of K). See also [**OS05**], which defines the contact invariant of a fibered link in M as an element of the Heegaard Floer homology of $-M$.

This will have the unfortunate effect that the orientation on a Heegaard torus associated to a grid diagram is opposite to the orientation on a Heegaard torus associated to a toroidal front diagram. This situation, though confusing, is unavoidable, since it is important to match the existing convention in the literature. To avert confusion, it will be convenient to define the notion of a *dual grid diagram* (Definition 4.2), a grid diagram for the mirror of a given link, K. In fact, after briefly recalling the original definition of a grid diagram of a link, we will thereafter work exclusively with dual grid diagrams — which may be canonically identified with toroidal front diagrams — throughout Section 4. We return to working with the original grid diagrams in Section 5, after we have proven a correspondence between planar subsets of toroidal fronts and planar fronts in Section 4.4. The coordinates on a dual grid diagram will always be the (θ_1, θ_2) coordinates inherited from the quotient map $S^3 \to L(p, q)$ described in the next section.

3. ξ_{UT} and toroidal front diagrams for lens spaces

3.1. Construction of ξ_{UT}. We begin with a construction of the universally tight contact structure ξ_{UT} on $L(p, q)$. Whenever we refer to the contact structure ξ_{UT} on $L(p, q)$ we will mean the isotopy class of the one constructed as follows.

Thinking of S^3 as the unit sphere in $\mathbb{C}^2$,

$$S^3 = \left\{ (u_1, u_2) \in \mathbb{C}^2 = \mathbb{C}_1 \times \mathbb{C}_2 \mid |u_1|^2 + |u_2|^2 = 1 \right\},$$

the standard tight contact structure on S^3 is given by (cf. [**Gei06**])

$$\xi_{st} = \ker \alpha,$$

where α is the 1-form

$$\alpha = r_1^2 \, d\theta_1 + r_2^2 \, d\theta_2$$

in terms of polar coordinates $(r_1, \theta_1) = u_1 \in \mathbb{C}_1$, $(r_2, \theta_2) = u_2 \in \mathbb{C}_2$. Thinking of S^3 as $\mathbb{R}^3 \cup \{\infty\}$, it is natural to identify the circle corresponding to $r_1 = 1$ with the z-axis $\cup \{\infty\}$ and the circle corresponding to $r_2 = 1$ with the unit circle on the xy-plane.

Let $\omega_p = e^{\frac{2\pi i}{p}}$. Then $L(p, q)$ can be identified as the quotient:

$$L(p, q) = S^3 / (u_1, u_2) \sim (\omega_p u_1, \omega_p^q u_2).$$

Noting that

$$\left\{ (r_1, \theta_1, r_2, \theta_2) \mid \theta_1 \in [0, 2\pi), \theta_2 \in \left[0, \frac{2\pi}{p}\right) \right\} \subset S^3$$

is a fundamental domain for the $\mathbb{Z}_p$ action of $\sim$, and that the coordinate r_2 may be recovered from the condition $r_1^2 + r_2^2 = 1$, we will specify points in $L(p, q)$ by

$$\left\{ (r_1, \theta_1, \theta_2) \mid r_1 \in [0, 1], \theta_1 \in [0, 2\pi), \theta_2 \in \left[0, \frac{2\pi}{p}\right) \right\}.$$

Let $\pi \colon S^3 \to L(p, q)$ be the covering map induced by the $\sim$ equivalence. Then $\xi_{\mathrm{UT}} = \pi_*(\xi_{\mathrm{st}})$ is a well-defined tight contact structure on $L(p, q)$, since the 1-form α is constant along tori of constant radius r_1 and the $\mathbb{Z}_p$ action is just translation in the θ_1 and θ_2 coordinates.

Note that the global 1-form α induces a co-orientation on ξ_{st} on S^3 and hence on ξ_{UT} on $L(p, q)$. The other universally tight contact structure on $L(p, q)$ (for $0 < q < p - 1$) may be obtained by using $-\alpha$ in the above construction. Regardless, most of this paper is insensitive to the co-orientation.

3.2. Toroidal front diagrams. Recall that a smooth link in a contact 3-manifold (M, ξ) is said to be *Legendrian* if its tangent vectors are everywhere tangent to the contact planes. A Legendrian isotopy is a smooth isotopy through Legendrian links, and the terminology *Legendrian link* refers to the Legendrian isotopy class of a Legendrian link as well as a specific representative.

The radial projection of a Legendrian link in $(L(p, q), \xi_{\mathrm{UT}})$ onto the radius $r_1 = \frac{1}{\sqrt{2}}$ Heegaard torus

$$\Sigma = \left\{ (r_1, \theta_1, \theta_2) \mid r_1 = \frac{1}{\sqrt{2}} \right\} \subset L(p, q)$$

gives a toroidal front diagram (defined below) on Σ from which we may recover the Legendrian link. Observe that Σ separates $L(p, q)$ into the two solid tori

$$V^\alpha = \left\{ (r_1, \theta_1, \theta_2) \mid r_1 \in \left[0, \frac{1}{\sqrt{2}}\right] \right\} \text{ and } V^\beta = \left\{ (r_1, \theta_1, \theta_2) \mid r_1 \in \left[\frac{1}{\sqrt{2}}, 1\right] \right\}$$

which are oriented so that $\Sigma = \partial V^\alpha = -\partial V^\beta$. (In terms of the standard surgery description of $L(p, q)$, we may view V^α as the surgered neighborhood and V^β as the exterior of the unknot in S^3.)

Remark 3.1. We use the notation α both to refer to the 1-form defining ξ_{st} and to sometimes mark an object as being in, or associated to, one of the two solid tori bounded by Σ. These two usages are common in the literature, and context should prevent confusion.

Points on Σ may be uniquely specified by the fundamental domain

$$\left\{ (\theta_1, \theta_2) \mid \theta_1 \in [0, 2\pi), \theta_2 \in \left[0, \frac{2\pi}{p} \right) \right\},$$

the intersection of a fundamental domain for $L(p, q)$ with Σ. Then with respect to the bases

$$\left\{ \frac{\partial}{\partial \theta_1}, \frac{\partial}{\partial \theta_2} \right\} \text{ and } \{d\theta_1, d\theta_2\}$$

for the tangent and cotangent space at each point, Σ is naturally parallelizable.

We are now ready to define toroidal front diagrams.

Definition 3.2. A *toroidal front diagram* (or simply a *toroidal front*) for a Legendrian link $\mathcal{L}$ in $(L(p, q), \xi_{\mathrm{UT}})$ is an immersion $f : S^1 \amalg \ldots \amalg S^1 \to \Sigma$ with the following properties:

- f is an embedding except at finitely many transverse double points and smooth except at finitely many cusps.
- The slopes $\frac{d\theta_2}{d\theta_1}$ of the tangent vectors at the smooth points satisfy $\frac{d\theta_2}{d\theta_1} \in (-\infty, 0)$.
- Each cusp is semi-cubical. See the discussion following Lemma 2.45 in [**Gei06**] for the precise definition of a semi-cubical cusp.

Proposition 3.3. *A toroidal front diagram uniquely specifies a Legendrian link up to Legendrian isotopy.*

Proof. Let γ be the image of f on Σ. We claim that γ is naturally the (θ_1, θ_2) projection of a Legendrian link in $(L(p, q), \xi_{\mathrm{UT}})$, where the r_1 coordinate is recovered from the Legendrian condition.

Set $m = \frac{d\theta_2}{d\theta_1}$. Then the condition that the vectors tangent to a Legendrian curve lie in $\ker \alpha$ implies that $r_1^2 \, d\theta_1 + (1 - r_1^2) \, d\theta_2 = 0$ and hence $\frac{r_1^2}{(r_1^2 - 1)} = m$. This gives the unique non-negative solution $r_1 = \sqrt{\frac{m}{m-1}}$. Because $m \in (-\infty, 0)$ at the smooth points of γ, we obtain $r_1 \in (0, 1)$ there. At the cusps, the one-sided tangencies agree, giving a slope $m \in (-\infty, 0)$ and hence a radius $r_1 \in (0, 1)$ there, too.

The condition that f is smooth away from the cusps ensures that the corresponding Legendrian link is smooth away from the preimages of the

cusps. The condition that the cusps of f are semi-cubical ensures that the Legendrian link is smooth in a neighborhood of the preimage of the cusps. □

Proposition 3.4. *Every Legendrian isotopy class of Legendrian links in $(L(p,q), \xi_{UT})$ has a representative admitting an associated toroidal front projection.*

Proof. The cores of the Heegaard solid tori V^α and V^β correspond to the circles where $r_1 = 0$ and 1, respectively. By a Legendrian isotopy, a Legendrian link may be made disjoint from these two cores. This ensures that the Legendrian link has a well-defined projection $\Pi\colon (r_1, \theta_1, \theta_2) \mapsto (\theta_1, \theta_2)$ to the Heegaard torus Σ. By a further Legendrian isotopy, we may ensure that the image of the projection is a smooth embedding except at finitely many transverse double points and finitely many cusps. Such Legendrian isotopies exist because the subspace of Legendrian representatives in a particular Legendrian isotopy class disjoint from the two cores and having a generic projection, as above, is open, dense, and positive dimensional. We claim that this projection is a toroidal front diagram for the Legendrian link.

Because each component of the Legendrian link is a smooth curve, its projection under Π is smooth except for where the link has a tangent vector that is parallel to $\frac{\partial}{\partial r_1}$. For the points where the projection is smooth, the Legendrian condition $r_1^2 \, d\theta_1 + (1 - r_1)^2 \, d\theta_2 = 0$ implies that $\frac{d\theta_2}{d\theta_1} \in (-\infty, 0)$ since $r_1 \in (0, 1)$. For the points where the projection is not smooth, the Legendrian condition $r_1^2 \, d\theta_1 + (1 - r_1)^2 \, d\theta_2 = 0$ implies that there are local coordinates for the projection presenting a neighborhood of the non-smooth point as a semi-cubical cusp [**Gei06**]. Since the projection is compact, there can only be finitely many cusps. □

Remark 3.5. Note that toroidal fronts for Legendrian links in lens spaces behave locally much like planar fronts for Legendrian links in $\mathbb{R}^3$. For example if two arcs a_1 and a_2 of a toroidal front transversally intersect at a point P with slopes m_1 and m_2, respectively, such that $-\infty < m_1 < m_2 < 0$, then the point projecting to P on a_1 lies above (has greater r_1 than) the point projecting to P on a_2. The correspondence between planar subsets of toroidal front projections (which represent Legendrian tangles in $(\mathbb{R}^3, \xi_{\text{st}})$) and standard planar front projections for Legendrian tangles in $(\mathbb{R}^3, \xi_{\text{st}})$ is made explicit in Section 4.4.

4. Grid diagrams and Legendrian knots

Let us quickly remind the reader of the definition of a toroidal grid diagram G_K for a link K in $L(p, q')$.

Definition 4.1. A *(twisted toroidal) grid diagram* G_K with grid number n for $L(p, q')$ consists of a five-tuple $(T^2, \vec{\alpha}, \vec{\beta}, \vec{\mathbb{O}}, \vec{\mathbb{X}})$, illustrated in Figure 2, where:

- T^2 is the standard oriented torus $\mathbb{R}^2/\mathbb{Z}^2$, identified with the quotient of $\mathbb{R}^2$ (with its standard orientation) by the $\mathbb{Z}^2$ lattice generated by the vectors $(1, 0)$ and $(0, 1)$.

- $\vec{\alpha} = \{\alpha_0, \ldots, \alpha_{n-1}\}$ are the n images α_i in $T^2 = \mathbb{R}^2/\mathbb{Z}^2$ of the lines $y = \frac{i}{n}$ for $i \in \{0, \ldots n-1\}$. Their complement $T^2 - \alpha_0 - \ldots - \alpha_{n-1}$ has n connected annular components, which we call the *rows* of the grid diagram.

- $\vec{\beta} = \{\beta_0, \ldots, \beta_{n-1}\}$ are the n images β_i in $T^2 = \mathbb{R}^2/\mathbb{Z}^2$ of the lines $y = -\frac{p}{q'}(x - \frac{i}{pn})$ for $i \in \{0, \ldots, n-1\}$. Their complement $T^2 - \beta_0 - \ldots - \beta_{n-1}$ has n connected annular components, which we call the *columns* of the grid diagram.

- $\vec{\mathbb{O}} = \{O_0, \ldots, O_{n-1}\}$ are n points in $T^2 - \vec{\alpha} - \vec{\beta}$ with the property that no two O's lie in the same row or column.
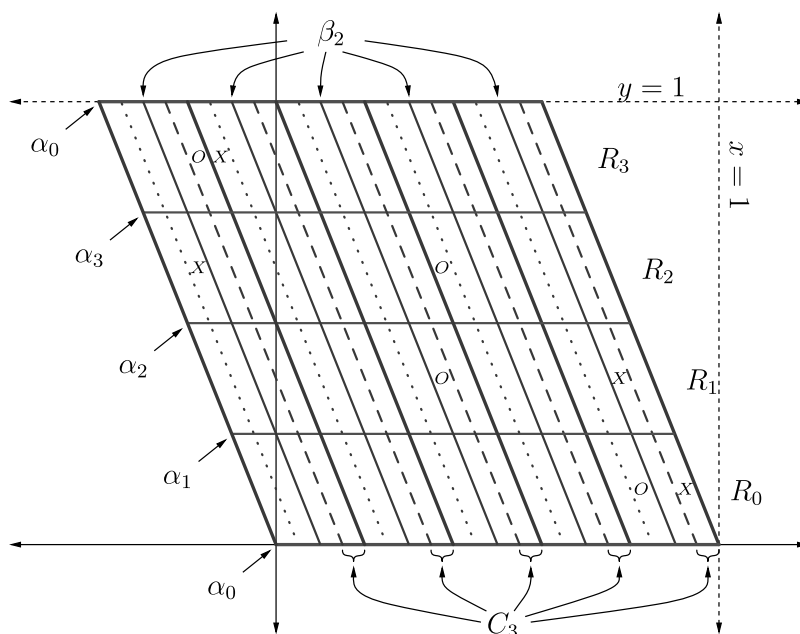
Figure 2. An example of a toroidal grid diagram G_K with grid number $n = 4$ for a link L in $L(5, 2)$. Here, C_3 is one of the four columns, while R_i are the rows.

- $\vec{\mathbb{X}} = \{X_0, \ldots, X_{n-1}\}$ are n points in $T^2 - \vec{\alpha} - \vec{\beta}$ with the property that no two X's lie in the same row or column.

We refer to the connected components of $T^2 - \vec{\alpha} - \vec{\beta}$ as the *fundamental parallelograms* of the grid diagram.

Two five-tuples $(T^2, \vec{\alpha}, \vec{\beta}, \vec{\mathbb{O}}, \vec{\mathbb{X}})_1$ and $(T^2, \vec{\alpha}, \vec{\beta}, \vec{\mathbb{O}}, \vec{\mathbb{X}})_2$ are equivalent (and, hence, represent the same grid diagram G_K) if there exists an orientation-preserving diffeomorphism $(T^2)_1 \to (T^2)_2$ respecting the markings (up to cyclic permutation of their labels).

One associates a unique (up to isotopy) oriented link K in $L(p, q')$ to a grid diagram $G_K = (T^2, \vec{\alpha}, \vec{\beta}, \vec{\mathbb{O}}, \vec{\mathbb{X}})$ as follows:

(1) First attach solid tori V^α and V^β to the torus T^2 so that $T^2 = \partial V^\alpha = -\partial V^\beta$, the α curves of G_K are meridians of V^α, and the β curves of G_K are meridians of V^β. This forms the standard embedding of T^2 with its decorations into $L(p, q')$.

(2) Connect each X_i to the unique O_j lying in the same row as X_i by an oriented "horizontal" arc embedded in that row of T^2, disjoint from the $\vec{\alpha}$ curves.

(3) Next, connect each O_j to the unique X_m lying in the same column as O_j by an oriented "slanted" arc embedded in that column of T^2, disjoint from the $\vec{\beta}$ curves.[1]

(4) The union of these two collections of n arcs forms an immersed (multi)curve γ in T^2. Remove all self-intersections of γ by pushing the interiors of the horizontal arcs slightly down into V^α and the interiors of the slanted arcs slightly up into V^β.

It will often be convenient to pick a particular fundamental domain for the grid diagram and "straighten" it out so that the image of the α curves are horizontal, the β curves are vertical, and each row is connected in the fundamental domain, as in Figure 3. From now on, we will always represent a grid diagram in this manner.

In accordance with Section 2, we make the following definition in order to identify a grid diagram for a link K in $L(p, q')$ with a Legendrian representative of the link in the contact manifold $(L(p, q), \xi_{\mathrm{UT}})$. As before, $qq' \equiv -1$ mod p.

Definition 4.2. Given a grid diagram G_K representing a link in $L(p, q')$, let G_K^* denote the *dual grid diagram*, obtained as follows and illustrated in Figure 4.

(1) Begin with any straightened fundamental domain for G_K.

---

[1]If an O_i and an X_j coincide, then we may take the slanted arc connecting them to be trivial joining with the horizontal arc to form a full circle.
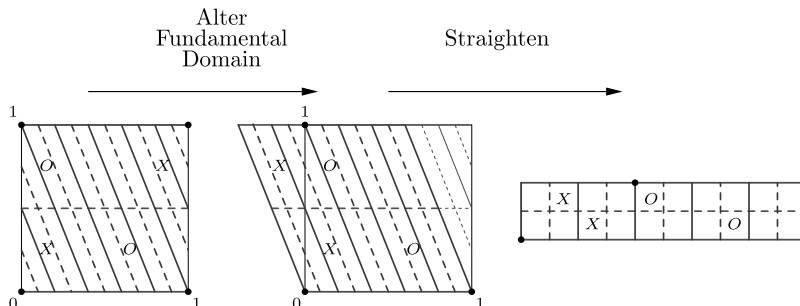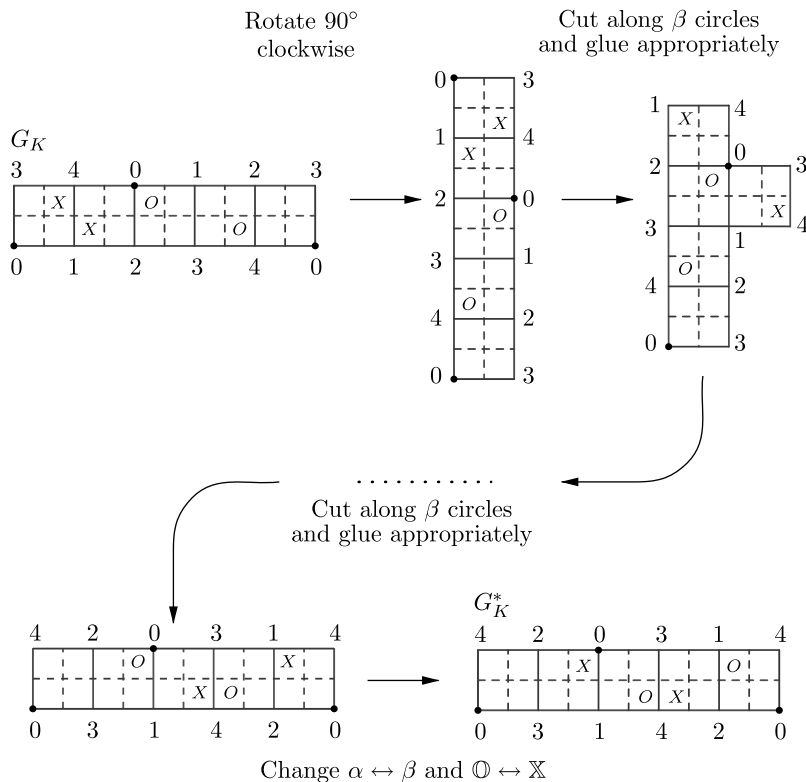
Figure 3. A grid number 2 diagram for a link in $L(5,2)$ is shown before and after straightening. One obtains the torus represented by the grid diagram G_K by identifying opposite edges of the square on the left-hand side in the standard manner. One can construct the same object, beginning with the rectangle on the right-hand side, by first identifying the two vertical edges and then the two boundary circles of the resulting annulus with an appropriate twist so that the thick black dots all represent the same point after the identifications.

(2) Rotate the fundamental domain 90° clockwise; the α curves of the old fundamental domain are now vertical, and the β curves are now horizontal.

(3) Chop the rotated fundamental domain along the newly horizontal arcs of the bottom-most β curve. Then reglue the resulting pieces together appropriately along the newly vertical arcs of the α curve on their sides. This produces a new straightened fundamental domain for the torus whose rows are connected.

(4) Relabel all horizontal circles on the torus as α circles and all vertical circles as β circles, and vice versa.

(5) Relabel all X's as O's and vice versa.

(6) The decorated, straightened fundamental domain represents G_K^*.

Note that G_K^* defines a link in $L(p,q)$, by the same procedure described above (connect X's to O's in each row and O's to X's in each column, with vertical passing over horizontal).

4.1. Identifying G_K^* with the constant radius Heegaard torus Σ. The torus arising in the definition of a grid diagram is, in fact, a Heegaard torus associated to a Heegaard decomposition of the appropriate lens space. Therefore, if we begin with a grid diagram G_K representing a link $K \subset L(p,q')$, then it is natural to identify the torus associated to the dual grid

Rotate 90°
clockwise

Cut along β circles
and glue appropriately

Cut along β circles
and glue appropriately

Change $\alpha \leftrightarrow \beta$ and $\mathbb{O} \leftrightarrow \mathbb{X}$

Figure 4. Constructing a dual grid diagram, G_K^*, from a grid diagram, G_K.

diagram, G_K^*, with the torus

$$\Sigma = \left\{ (r_1, \theta_1, \theta_2) \mid r_1 = \frac{1}{\sqrt{2}}, \theta_1 \in [0, 2\pi), \theta_2 \in \left[0, \frac{2\pi}{p}\right) \right\} \subset L(p, q)$$

defined in Section 3.2 (where the coordinates give an implicit choice of fundamental domain for Σ) so that each horizontal α curve of slope 0 corresponds to a circle of constant θ_2 and that each slanted β curve of slope $-\frac{p}{q}$ corresponds to a circle of constant θ_1 taken mod $\frac{2\pi}{p}$. (In the fundamental domain the β curves correspond to a union of the p lines in Σ with θ_1 coordinate in the set $\mathbf{a} = \left\{ a + \frac{2\pi k}{p} \right\}$, for $k \in \{0, \ldots p-1\}$ and some fixed $a \in \left[0, \frac{2\pi}{p}\right)$.) In particular, the α curves are meridians of V^α and the β curves are meridians of V^β.

We choose the identification of T^2 with Σ such that, within each row, the unique O and X have the same θ_2 coordinate and, within each column, the unique O and X have the same θ_1 coordinate mod $\frac{2\pi}{p}$. Furthermore, if a pair of an O and an X lie in the same fundamental parallelogram,

then it is natural to associate to the pair a trivial Legendrian unknot.[2] In what follows, we may therefore assume, without loss of generality, that no fundamental parallelogram contains both an X and an O.

Remark 4.3. It is worthwhile to remark at this point that there is a natural correspondence between Legendrian links in $(L(p, q), \xi_{\mathrm{UT}})$ and $\mathbb{Z}_p$-symmetric Legendrian links in (S^3, ξ_{st}) obtained via the covering operation. This correspondence matches the correspondence between grid diagrams G_K for $K \subset L(p, q)$ and their lifts to grid diagrams $G_{\widetilde{K}}$ for $\widetilde{K} \subset S^3$. See [**BGH08**].

We are now ready to state and prove the main theorem. Statements and proofs of many of the supporting lemmas and propositions occupy the remainder of this section:

Theorem 4.4. *Associated to a grid diagram for a link K in the lens space $L(p, q')$ is a unique Legendrian representative $\mathcal{L}_K$ of the topological mirror $m(K)$ with respect to $(-L(p, q'), \xi_{UT})$. Conversely, every Legendrian link $\mathcal{L}_K$ in $(-L(p, q'), \xi_{UT})$ representing $m(K)$ can be specified by means of a grid diagram for K in $L(p, q')$.*

Proof. Let q satisfy $qq' \equiv -1 \mod p$ (see Section 2 for a discussion of orientation conventions). Beginning with G_K, a grid diagram for $K \subset L(p, q')$, we produce the dual grid diagram G_K^* associated to $m(K) \subset L(p, q)$ using the procedure described in Definition 4.2. Lemma 4.5 then explains how to obtain a toroidal front from a rectilinear projection associated to G_K^*, and Proposition 3.3 associates a unique Legendrian link in $(L(p, q), \xi_{\mathrm{UT}})$ to this toroidal front on Σ, a coordinatized Heegaard torus for $L(p, q)$. Proposition 4.6 then proves that the choice of rectilinear projection does not affect the Legendrian isotopy class of the resulting Legendrian link.

Conversely, if we begin with a Legendrian link $\mathcal{L}_K$ representing $m(K) \subset L(p, q)$, Proposition 3.4 associates to it a toroidal front on Σ. Lemma 4.8 then explains how to obtain a grid diagram G_K^* representing $m(K)$ in $L(p, q)$ from the toroidal front. By reversing the procedure described in Definition 4.2, one obtains a grid diagram G_K representing K in $L(p, q')$. $\square$

4.2. Constructing a toroidal front from a grid diagram. To a grid number n grid diagram we can associate 2^{2n} possible piecewise linear projections to T^2 (there are two choices for each of the $2n$ horizontal and vertical arcs). We will call any such projection a *rectilinear projection.*

Lemma 4.5. *A rectilinear projection associated to a grid diagram G_K^* for a link $K \subset L(p, q)$ uniquely specifies a toroidal front for $\mathcal{L}_K$, a Legendrian link in $(L(p, q), \xi_{UT})$.*

---

[2]More precisely, one isotops the component to lie in a Darboux ball and chooses the Legendrian isotopy class contactomorphic to the $\mathrm{tb} = -1$ unknot in (S^3, ξ_{st}).
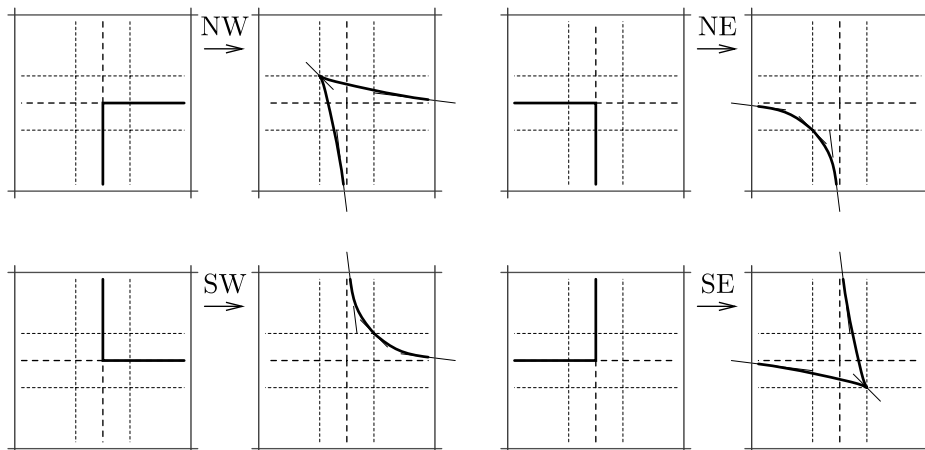
Figure 5. The smoothings and cuspings of corners in the rectilinear projection associated to a grid diagram G_K on Σ.

Proof. We continue to view the grid diagram G_K^* on Σ as described in Section 4.1. Recall that we have chosen the identification so that the O and X in each row have the same θ_2 coordinate and the O and X in each column have the same θ_1 coordinate mod $\frac{2\pi}{p}$.

To obtain a diagram for the link K on Σ corresponding to G_K^*, we may join each O and X in a row by a horizontal arc of constant θ_2 and join each O and X in a column by a vertical arc of constant θ_1 mod $\frac{2\pi}{p}$.

We now perturb this rectilinear projection to yield a toroidal front projection as follows. The corners of the rectilinear diagram coincide with the O's and X's. Replace each NW and SE corner with a semi-cubical cusp just outside the corner; replace each NE and SW corner with a rounding just inside the corner. See Figure 5. These may be done so that they are tangent to the induced line field (of slope -1) on Σ and so that the associated Legendrian curve intersects Σ near the original O's and X's. Furthermore, the smoothed and cusped corners may now be joined by curves with finite negative slopes (in $(-\infty, -1]$ for corners in a column and in $[-1, 0)$ for corners in a row) producing a toroidal front. These choices may be made so that the toroidal front is arbitrarily close to the original rectilinear projection. Furthermore, the toroidal front isotopy class of the result is unique. □

By Proposition 3.3, there is a Legendrian link associated to the front obtained above. Figure 6 shows two toroidal front diagrams obtained by smoothing two rectilinear projections obtained from the same grid diagram.
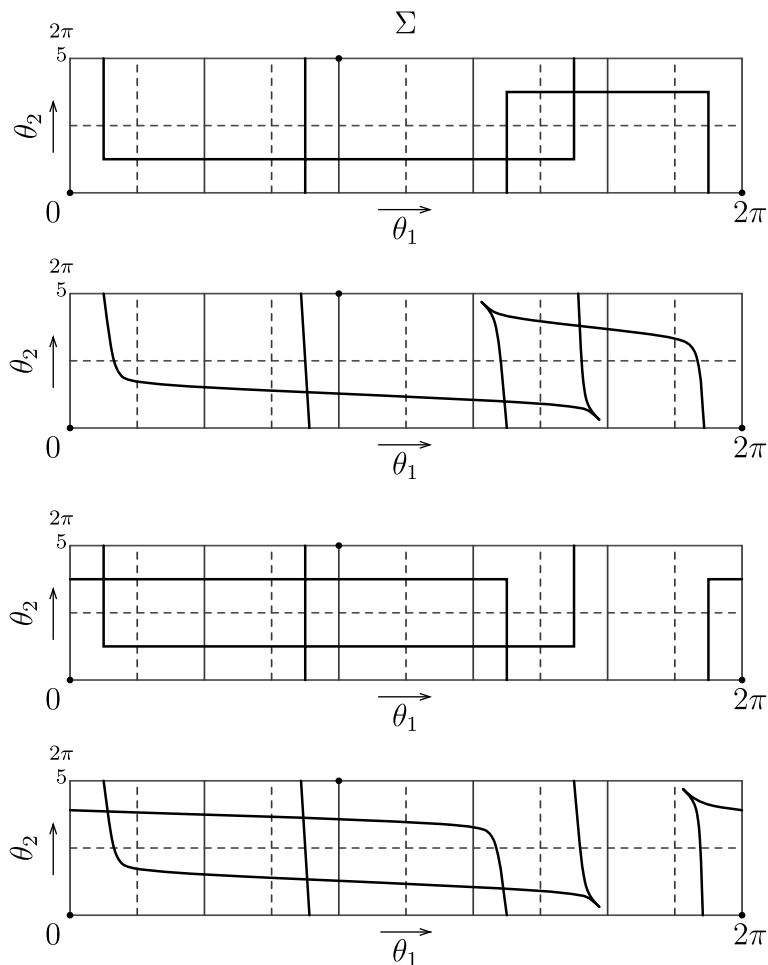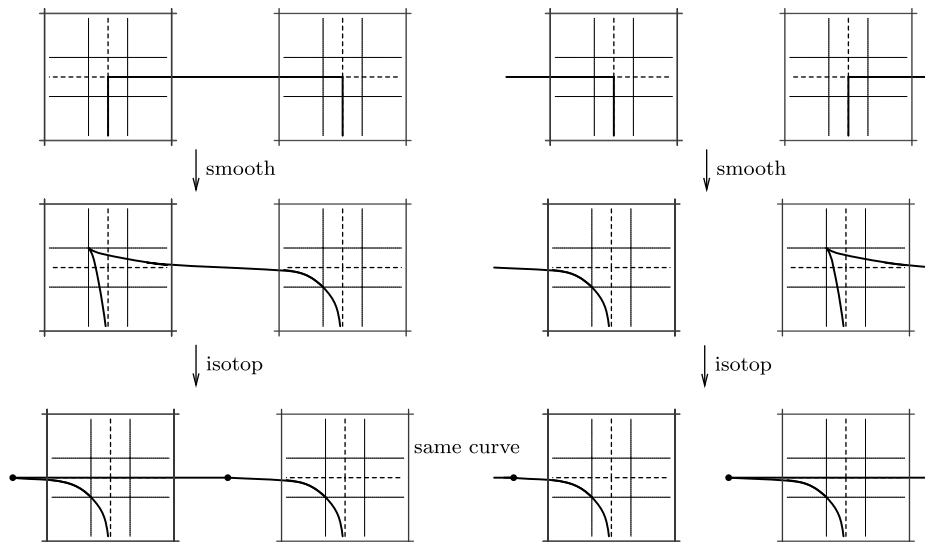
Figure 6. Here are two rectilinear projections for the same grid diagram of grid number 2 for $L(5, 2)$ and their associated toroidal front diagrams on Σ.

4.3. Legendrian isotopy class invariance of constructed toroidal front.

Proposition 4.6. *The Legendrian isotopy class of the link obtained from a grid diagram G_K^* does not depend upon the choice of rectilinear projection used to define the toroidal front.*

Proof. It suffices to show that the toroidal fronts obtained from two rectilinear projections differing in a single row represent Legendrian isotopic links; the case for columns is completely analogous. The top rows of Figures 7 and 8 show the two choices of horizontal arcs for an O and an X

Figure 7. The left- and right-hand sides of this figure show
the Legendrian isotopy equivalence of the Legendrian curves
obtained from the two choices of horizontal arc in the recti-
linear projection connecting an O and an X in a row of a grid
diagram. The rectilinear projections on the upper level may
both be smoothed to toroidal fronts as in the middle level.
These two toroidal fronts can be moved by toroidal front iso-
topies to diagrams (bottom row) which, though not toroidal
fronts, represent the same, smooth Legendrian link.

in a row in a rectilinear projection. Figure 7 shows when the vertical arcs
are incident to the horizontal arcs from the same side; Figure 8 shows when
the vertical arcs are incident to the horizontal arcs from opposite sides. The
middle rows illustrate the corresponding toroidal fronts obtained from the
rectilinear projections as in Lemma 4.5.

A toroidal front isotopy naturally induces a Legendrian isotopy of the cor-
responding Legendrian link; we proceed by moving the two toroidal fronts,
by toroidal front isotopies, to limiting diagrams which, though not toroidal
fronts, still represent the same smooth Legendrian link. These two diagrams,
pictured in the bottom rows of Figures 7 and 8, both naturally represent
a Legendrian link which passes through the core of the solid torus. The
projection has slope $\frac{d\theta_2}{d\theta_1} = 0$ at the two black dots, p_1, p_2, which are posi-
tioned at distance $\theta_1 = \pi$ away from each other on Σ. In other words, in
both diagrams, the entire horizontal arc connecting p_1 and p_2 represent a
single point, p, on the core of the solid torus, and the points near p_1 and p_2
with non-zero slope are the projections of points nearby p (which project to
opposite sides of the Heegaard torus, as pictured). This Legendrian link will
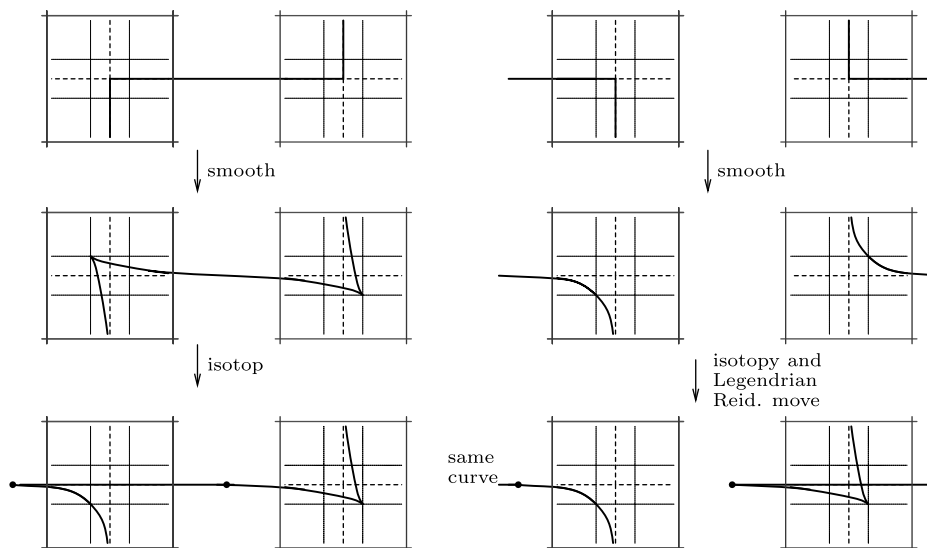
Figure 8. See the caption for Figure 7. To pass from the rightmost middle row to the bottom row, one needs to use a local Legendrian Reidemeister I move (see Section 5) in addition to a toroidal front isotopy. See Figure 9 for more details.
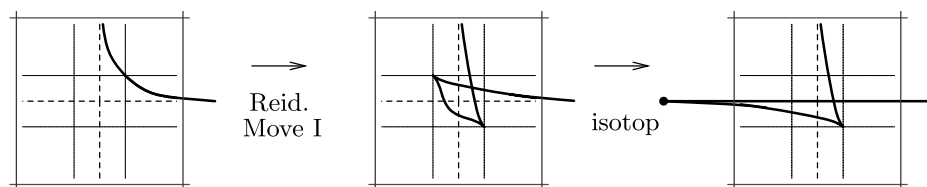
Figure 9. An intermediate isotopy of the lower two right-hand regions of Figure 8 is through a Legendrian Reidemeister I move.

be smooth at all points away from p, since the toroidal front projection is smooth at all points away from p_1, p_2. To ensure that the Legendrian link is smooth at p, one need only arrange for all higher order derivatives of θ_2 with respect to θ_1 to match at p_1, p_2, which can be done by smooth toroidal front isotopy.

Different choices of horizontal or vertical arcs thus produce toroidal fronts of Legendrian isotopic Legendrian links.   □

Remark 4.7. It is natural to view a rectilinear projection for a Legendrian link as a front diagram for a certain bivalent Legendrian graph whose smoothings produce the toroidal fronts we have been discussing. Note that

radial arcs in $L(p, q)$, i.e., those whose tangent vectors satisfy $\frac{\partial}{\partial \theta_1} = \frac{\partial}{\partial \theta_2} = 0$, are Legendrian. Therefore, a grid diagram defines a bivalent Legendrian graph made up of a union of radial trajectories between the cores of the two solid tori, passing through Σ at the $2n$ basepoints. A horizontal arc on Σ has slope 0, and thus the points of its interior all define a single point on the core of V^α at radius $r_1 = 0$, irrelevant θ_1, and specified θ_2. Similarly a vertical arc has slope ∞ and thus the points of its interior all define a single point on the core of V^β at radius $r_1 = 1$, specific $\theta_1 \bmod \frac{2\pi}{p}$, and irrelevant θ_2. At the endpoints of these horizontal and vertical arcs are the O's and X's. Since the one-sided tangencies at these points sweep through negative slopes between horizontal and vertical, these points define the radial Legendrian arcs.

To complete the correspondence between grid diagrams and Legendrian links, we now need only show that any toroidal front diagram is isotopic, through toroidal fronts, to one obtained from a grid diagram:

Lemma 4.8. *Given a toroidal front diagram on Σ, there exists a grid diagram G_K^* representing the associated Legendrian link.*

Proof. Let γ be a toroidal front on Σ. Perturb γ slightly by a toroidal front isotopy so that all tangencies of slope -1 are isolated. If γ has a tangency of slope -1 at a non-cusp point with neighboring points having slopes either all strictly greater than -1 or all strictly less than -1, then a slight isotopy of γ in this neighborhood will eliminate the -1 sloped tangency. Isotop to remove all such tangencies. Thus on the arcs along γ between consecutive tangencies of slope -1 and cusps, the tangencies to γ have slopes in the range $(-\infty, -1)$ or $(-1, 0)$.

Similarly, if γ has a cusp with neighboring points having slopes either all strictly greater than -1 or all strictly less than -1, then we may arrange, via a slight isotopy, that γ instead looks locally like Figure 10 near the cusp. As a consequence, the tangency at each cusp has slope -1. Furthermore, if
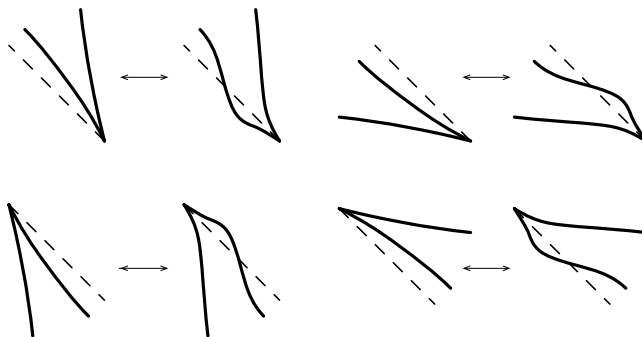
Figure 10. Arrange cusps by Legendrian isotopies to have slope -1.

p is a point of γ whose tangent has slope -1, then points on γ near p to one side have slopes > -1, and points near p to the other side will have slopes < -1.

Mark each tangency of slope -1. We will refer to consecutive markings as a *horizontal pair* if the arc of γ joining them has slopes in the range $(-1, 0)$; similarly, we will call consecutive markings a *vertical pair* if the arc joining them has slopes in the range $(-\infty, -1)$. Arrange, by toroidal front isotopy, that the arc joining each horizontal pair is very close to slope 0.

It is now straightforward to approximate the toroidal front by a rectilinear projection composed of horizontal and vertical segments in such a way that the associated toroidal front smoothing is isotopic, through toroidal fronts, to the original toroidal front. Note that each horizontal pair can be approximated by a single horizontal segment, while the vertical pairs may be approximated by zig-zags which, when perturbed to yield a toroidal front diagram, produce no cusps. $\square$

4.4. Constructing a planar front from a grid diagram. For K a link in S^3, Ozsváth *et al.* [**OST06**] describe how one associates to a grid diagram G_K for K a standard planar front diagram for a Legendrian representative of the topological mirror of K, $m(K)$. In this section, we prove that the planar front diagram described in [**OST06**] can actually be viewed as a toroidal front diagram supported in a planar region on the Heegaard torus for S^3 with the reverse orientation. As a straightforward consequence of our argument, one can associate to any planar subset of a toroidal front diagram a planar front diagram representing a Legendrian tangle in (B^3, ξ_{st}). This will be of use in defining Legendrian Reidemeister moves for lens spaces, as we do in Section 5.

Let G_K be a grid diagram for $K \subset S^3$ and G_K^* the grid diagram for $m(K) \subset -S^3$. By distinguishing an α curve and a β curve on G_K^*, we may choose the horizontal and vertical arcs connecting the X's and O's so that they are disjoint from the two distinguished curves. (This may be done since each α and β curve on a genus 1 Heegaard diagram for S^3 intersect just once.) We thus obtain a toroidal projection that is confined to a planar subset of the torus. By the results of the previous section, we know that the Legendrian isotopy class of the knot is unaffected by this choice. See Figure 11.

We may assume that our distinguished α and β curves correspond to the circles $\theta_2 = \pm\pi$ and $\theta_1 = \pm\pi$ on the Heegaard torus, so that all the basepoints of our grid diagram have coordinates $(\theta_1, \theta_2) \in (-\pi, \pi) \times (-\pi, \pi)$. After smoothing to obtain a toroidal front for the Legendrian link associated to the grid diagram, any tangency is neither horizontal nor vertical. Then using our familiar coordinates $(r_1, \theta_1, \theta_2)$ for points in S^3, our Legendrian link is supported in the open tetrahedron

$$W = \{(r_1, \theta_1, \theta_2) \mid r_1 \in (0, 1), \theta_1 \in (-\pi, \pi), \theta_2 \in (-\pi, \pi)\}.$$
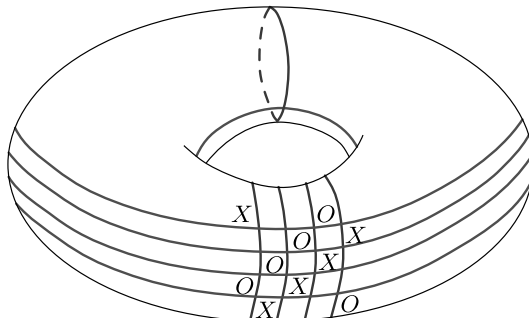
Figure 11. A grid diagram whose basepoints are supported in a small planar region of the Heegaard torus.

The map $f\colon W \to \mathbb{R}^3$ defined by

$$f(r_1, \theta_1, \theta_2) = \left(\frac{1}{2}(\theta_1 - \theta_2),\, 1 - 2r_1^2,\, \frac{1}{2}(\theta_1 + \theta_2) \right)$$

induces a contactomorphism from $\xi_{\mathrm{st}}|W$ to $\xi_{\mathbb{R}^3}|f(W)$. Recall $\xi_{\mathrm{st}} = \ker(r_1^2 d\theta_1 + (1 - r_1^2)\, d\theta_2)$ is the standard contact structure on S^3 (and hence on W) while $\xi_{\mathbb{R}^3} = \ker(dz - y\, dx)$ is the standard contact structure on $\mathbb{R}^3$.

The square $W_{r_1 = 1/\sqrt{2}}$ that is the complement of the distinguished α and β curves is mapped to the open diamond in the xz-plane of $\mathbb{R}^3$ with vertices at $(\pm\pi, 0, 0)$ and $(0, 0, \pm\pi)$. In this manner the map f carries a toroidal front for a Legendrian link in S^3 to a standard front for a Legendrian link in $\mathbb{R}^3$. Indeed, the image $f(W)$ is the open rectangular solid obtained by sweeping this open diamond in the xz-plane along the interval $(-1, 1)$ of the y-axis.

By Legendrian isotopies, we may arrange that any Legendrian link in $\mathbb{R}^3$ is contained in $f(W)$. Accordingly, by scaling and vertical compression, we may arrange a front to be contained within this diamond, so that every tangent line has slope in the range $(-1, 1)$. Hence (after any necessary scaling and compression) the map f^{-1} carries a front for a Legendrian link in $\mathbb{R}^3$ to a toroidal front.

In other words, f sends our toroidal front to a standard planar front. Up to planar front isotopy, this is equivalent to rotating the planar subset of the toroidal front $45°$ counterclockwise. To verify that our construction matches the one desribed in [**OST06**], begin by rotating a planar rectilinear projection for G_K $90°$ clockwise to produce a planar rectilinear projection for G_K^*. This has the effect of changing all crossings of the associated link. Then rotate the toroidal front $45°$ counterclockwise to produce a planar front. This is precisely the procedure described in [**OST06**].

5. Topological and Legendrian equivalence under grid moves

Now that we have established a relationship between a grid diagram G_K for a link $K \subset L(p, q')$ and a Legendrian representative $\mathcal{L}_K$ of K in $(L(p, q), \xi_{\text{UT}})$, we turn to the question of the uniqueness of this representation. Our goal is to provide an elementary set of moves, as in [**Cro95**, **MOST06**, **OST06**], allowing one to move between any two grid diagram representatives of the same topological or Legendrian knot type.

The main theorem of this section is the following:

Theorem 5.1. *Let G_K and G'_K be grid diagrams representing smooth links K and K' in $L(p, q')$ (resp., Legendrian links $\mathcal{L}_K$ and $\mathcal{L}_{K'}$ in $(L(p, q), \xi_{\text{UT}})$).*

(1) *K and K' are smoothly isotopic if and only if there exists a sequence of elementary topological grid moves connecting G_K to G'_K.*

(2) *$\mathcal{L}_K$ and $\mathcal{L}_{K'}$ are Legendrian isotopic if and only if there exists a sequence of elementary Legendrian grid moves connecting G_K to G'_K.*

Figures 12–14 illustrate the elementary topological grid moves: (de)stabilizations and commutations. These moves look locally like those described in [**OST06**] for S^3 knots. The elementary Legendrian grid moves form a subset of the elementary grid moves, including commutations and (de)stabilizations of types X:NW, X:SE, O:NW, O:SE. We will say that two grid diagrams are topologically (resp., Legendrian) grid-equivalent if they are related by a finite sequence of elementary topological (resp., Legendrian) grid moves.

Proof Item 1: Smooth isotopy. The Reidemeister theorem for links in S^3 states that two links are smoothly isotopic if and only if their planar projections are related by planar isotopies and Reidemeister moves. Since each such move corresponds to a local isotopy (supported in $\mathbb{R}^3$), it is immediate that grid-equivalent grid diagrams for links in lens spaces represent smoothly isotopic links. Furthermore, the observation that all Reidemeister moves are local, coupled with the natural correspondence between planar subsets of toroidal projections of lens space links and standard planar projections of tangles in $\mathbb{R}^3$, immediately implies a version of Reidemeister's theorem for lens space links:
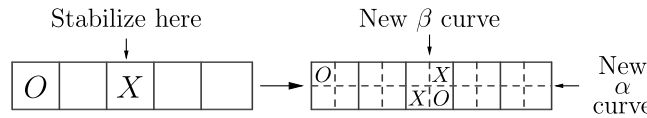
Figure 12. An illustration of a NW stabilization at an X basepoint for a grid number 1 knot in $L(5, 1)$. One introduces new α–β and X–O pairs in the rectangle specified by the chosen basepoint. A destabilization is the inverse of this operation.

New β curve

New
α →
curve
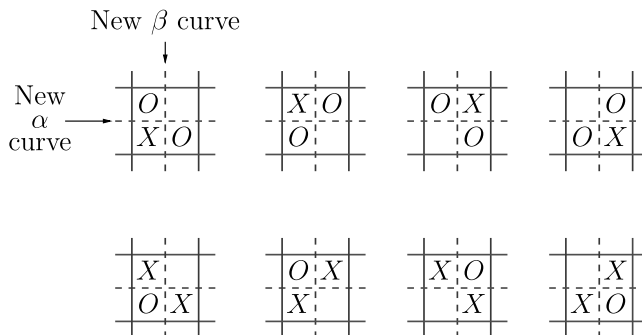
Figure 13. Local pictures for all eight different types of stabilizations. Starting from the left on the top row, these are denoted O:NE, O:SE, O:SW, and O:NW. Along the bottom row, we have X:NE, X:SE, X:SW, and X:NW.
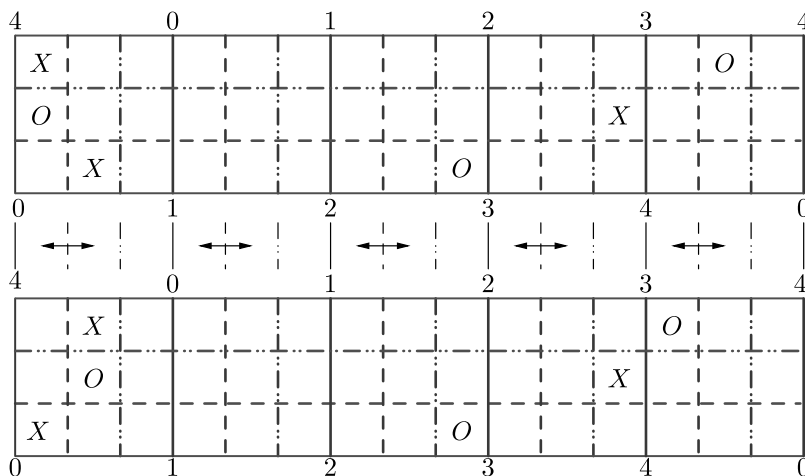
Figure 14. A before (top) and after (bottom) snapshot of a first and second column commutation on a grid number 3 diagram for a link in $L(5,1)$. Since the basepoint pairs in these columns do not interleave, we can exchange the markings as shown. A row commutation is the obvious analog for two adjacent rows. In general, a row or column commutation can be performed on any two adjacent rows or columns as long as the markings in the two columns do not interleave.

Proposition 5.2. *Two smooth links K_1 and K_2 in $L(p,q)$ are smoothly isotopic if and only if their toroidal projections are related by a sequence of smooth isotopies and Reidemeister moves $I, II, III,$ and IV, picture in Figure 15.*
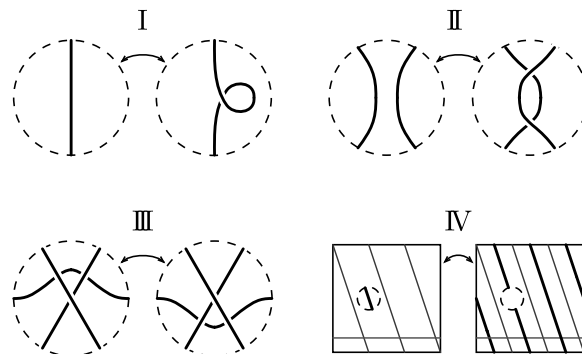
Figure 15. An illustration of the lens space Reidemeister moves. Moves I, Ⅱ, Ⅲ look locally like the S^3 Reidemeister moves, but should be thought of here as occurring in a sufficiently small disk on the Heegaard torus. Move Ⅳ corresponds to replacing an arc of the boundary of a meridional disk (in either solid handlebody) with the complementary arc. Here, we have pictured this move for a meridional disk in V^β in the lens space $L(3,1)$.

To prove that any two smoothly isotopic links K_1 and K_2 have topologically grid-equivalent grid diagrams, we use the argument outlined by Dynnikov in [**Dyn06**]. First, we represent K_1 and K_2 by (rectilinear) toroidal projections, using Lemma 4.2 of [**BGH08**]. By the Reidemeister theorem for lens space links, we can move from one toroidal projection to the other by a sequence of smooth isotopies and moves of type I–Ⅳ. By the same arguments used in the proofs of Lemma 4.2 and Proposition 4.3 of [**BGH08**], we can approximate each stage of this process using a grid diagram. Provided that each intermediate step is sufficiently simple (subdivide the compact isotopy further if not), it is easy to verify that each step can be accomplished using elementary grid moves. Reidemeister move Ⅳ does not require a grid move; rather, one chooses an alternative projection of the link to the Heegaard torus. Figures 16–18 enumerate all possible versions of the other Reidemeister moves, indicating how they can be obtained via grid moves.
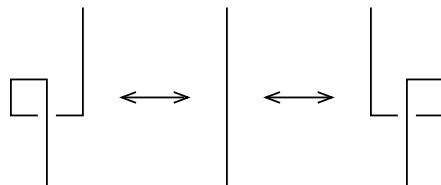
Figure 16. Reidemeister I via grid moves.
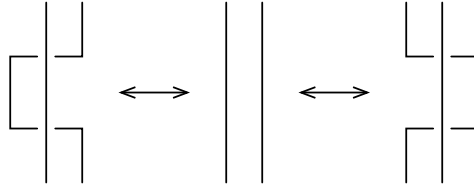
Figure 17. Reidemeister II via grid moves.
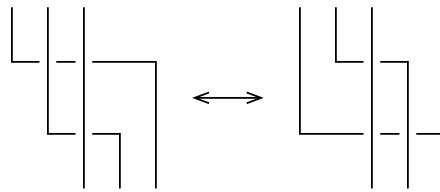
Figure 18. Reidemeister III via grid moves.

Item 2: Legendrian isotopy. In [**Świ92**], Swiatkowski proves that two Legendrian links in S^3 are Legendrian isotopic if and only if their corresponding planar fronts are related by a sequence of planar isotopies and Legendrian Reidemeister moves as in Figure 19. Since each of his Reidemeister moves corresponds to a local Legendrian isotopy (i.e., takes place in a Darboux ball), his result will immediately imply that Legendrian grid-equivalent grid diagrams represent Legendrian-isotopic lens space links, once we understand the relationship between planar subsets of toroidal fronts and standard planar fronts. This relationship, explained in detail in Section 4.4, coupled with Swiatkowski's result, yields a Legendrian Reidemeister theorem for Legendrian links in $(L(p,q), \xi_{\mathrm{UT}})$:
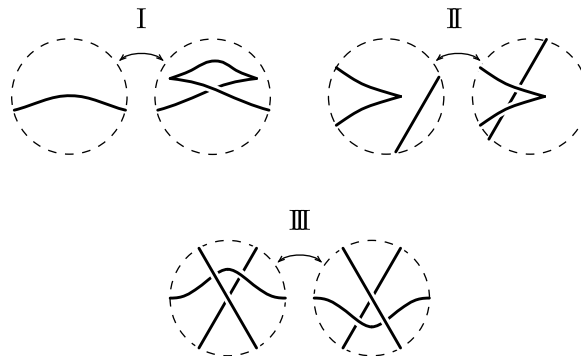
Figure 19. Legendrian Reidemeister moves for planar fronts.
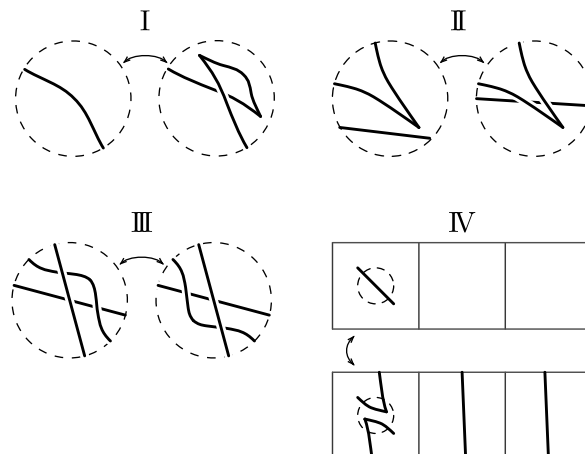
Figure 20. Legendrian Reidemeister moves for toroidal fronts.

Proposition 5.3. *Two toroidal front diagrams represent Legendrian-isotopic links in $(L(p,q), \xi_{UT})$ if and only if they can be connected by a sequence of toroidal front isotopies, Legendrian Reidemeister moves, and Legendrian slides across meridional disks (which we will call Legendrian Reidemeister moves of type IV), as in Proposition 4.6.*

The Legendrian Reidemeister moves I–IV on a toroidal front are illustrated in Figure 20.

To prove that Legendrian-isotopic links K_1 and K_2 have Legendrian grid-equivalent grid diagrams, one first uses Proposition 3.4 to represent both by toroidal fronts on Σ. By the Legendrian Reidemeister theorem for links in lens spaces, we can move between the two fronts by a sequence of toroidal front isotopies and Legendrian Reidemeister moves. An argument exactly as in the proof of Lemma 4.8 produces a dual grid diagram $G^*_{K_i}$ for each stage of the Legendrian isotopy. It is then straightforward, using arguments analogous to those given in the verification of topological grid equivalence, to show that the associated grid diagrams G_{K_i} (*not* the dual grid diagrams $G^*_{K_i}$) associated to each stage of the Legendrian isotopy are Legendrian grid equivalent. □

6. The Thurston–Bennequin invariant and bounds on grid number

Let $\mathcal{L}_K$ be an oriented Legendrian link in a contact rational homology sphere (Y, ξ) repesenting the topological oriented link K with components $K_1, \ldots, K_\ell$. We begin by defining the Thurston–Bennequin number, $\mathrm{tb}(\mathcal{L}_K)$, a classical Legendrian invariant. Traditionally tb is defined when K is a null-homologous link in a contact 3-manifold, see, e.g., [**FT97**]. The definition

extends in a natural way to rationally null-homologous oriented links. Please see [**Özt05**] for an alternative approach.

6.1. Contact framing, Seifert framing, and the Thurston–Bennequin number. Let $N(K)$ denote a small tubular neighborhood of the link K with $N(K_i)$ denoting the component that is a neighborhood of K_i. Let μ_i be an oriented meridian of the closure of $N(K_i)$ so that it links K_i once positively. Typically, a framing for K_i is a choice of a slope on $\partial N(K_i)$ that algebraically intersects the meridian μ_i once. We shall relax this notion of framing so that it may be a collection of parallel slopes on $\partial N(K_i)$ that each algebraically intersect the meridian μ_i a fixed number of times.

The Thurston–Bennequin number $\mathrm{tb}(\mathcal{L}_K)$ measures the discrepancy between the *contact framing* and the *Seifert framing* of the oriented Legendrian link $\mathcal{L}_K$.

Definition 6.1. The *contact framing* for $\mathcal{L}_K$ is the tuple

$$\boldsymbol{\gamma} = ([\gamma_1], \ldots, [\gamma_\ell]) \in \bigoplus_{i=1}^{\ell} H_1(T_i^2; \mathbb{Z})$$

defined by pushing the oriented components K_i of K into $T_i^2 = \partial(Y - N(K_i)) \subset \partial(Y - N(K))$ along the contact planes.

Definition 6.2. The *Seifert framing* for K is the tuple

$$\boldsymbol{\lambda} = ([\lambda_1], \ldots, [\lambda_\ell]) \in \bigoplus_{i=1}^{\ell} H_1(T_i^2; \mathbb{Z})$$

such that

(1) λ_i is a collection of parallel, coherently oriented, simple closed curves on $T_i^2 = \partial N(K_i)$,
(2) $\mu_i \cdot \lambda_i = d$ for each i, where d is the order of $[K] \in H_1(Y; \mathbb{Z})$, and
(3) via the induced maps on homology coming from the inclusions $T_i^2 \hookrightarrow Y - N(K)$, we have $\sum_{i=1}^{\ell} \lambda_i = 0 \in H_1(Y - N(K); \mathbb{Z})$.

It is clear that the contact framing is well defined, but it may not be so clear that the Seifert framing is well defined for non-nullhomologous oriented links in rational homology spheres.

Lemma 6.3. *The Seifert framing is well defined.*

Proof. To simplify notation, curves will be identified with the homology classes they represent in various spaces.

Given an oriented link $K = K_1 \cup \cdots \cup K_\ell$ in a rational homology sphere Y with oriented meridians μ_i as above, observe that $H_1(Y - N(K); \mathbb{Q}) \cong$

$\mathbb{Q}^\ell$. Moreover, the homology classes of the oriented meridians form a basis $\{\mu_1, \ldots, \mu_\ell\}$. Set

$$\boldsymbol{\mu} = (\mu_1, \ldots, \mu_\ell) \in \bigoplus_{i=1}^{\ell} H_1(Y - N(K); \mathbb{Q}).$$

We construct the Seifert framing as follows. For each component K_i of K pick an oriented push-off, λ_i', of K_i on $\partial N(K_i)$. Note that λ_i' is a framing in the usual sense. Write

$$\boldsymbol{\lambda}' = (\lambda_1', \ldots, \lambda_\ell') \in \bigoplus_{i=1}^{\ell} H_1(Y - N(K); \mathbb{Q}).$$

Since each λ_i' may be expressed as a $\mathbb{Q}$-linear combination of the μ_j, there exists an $\ell \times \ell$ matrix A with rational coefficients such that

$$\boldsymbol{\lambda}' = A\boldsymbol{\mu}.$$

Let d be the smallest positive integer such that dA has integral coefficients, and let $\boldsymbol{\lambda}^\Sigma$ denote the image of $\boldsymbol{\lambda}$ under the natural map

$$\bigoplus_{i=1}^{\ell} H_1(Y - N(K); \mathbb{Z}) \to H_1(Y - N(K); \mathbb{Z})$$

which sends

$$(\lambda_1, \ldots, \lambda_\ell) \mapsto \sum_{i=1}^{\ell} \lambda_i.$$

Then, we see that

$$d\boldsymbol{\lambda}'^\Sigma - d(A\boldsymbol{\mu})^\Sigma = 0 \in H_1(Y - N(K); \mathbb{Z}).$$

Furthermore, by collecting like terms, one produces a unique element

$$\boldsymbol{\lambda} = (\lambda_1, \ldots, \lambda_\ell) \in \bigoplus_{i=1}^{\ell} H_1(T_i^2; \mathbb{Z}).$$

More precisely,

$$\lambda_i = d\left(\lambda_i' - \sum_{j=1}^{\ell} A_{ji}\mu_i\right).$$

To see that the resulting element of $\bigoplus_{i=1}^{\ell} H_1(T_i^2; \mathbb{Z})$ is independent of the original choices of the push-offs λ_i', simply note that for each K_i, any other choice λ_i'' will be related to the λ_i' by $\lambda_i'' = \lambda_i' + k_i\mu_i$ for some $k_i \in \mathbb{Z}$. The corresponding matrix A'' is given by

$$A_{ji}'' = \begin{cases} A_{ji} & \text{for } i \neq j \\ A_{ii} + k_i & \text{for } i = j. \end{cases}$$

Hence

$$\lambda_i'' - \sum_j A_{ji}'' \mu_i = \lambda_i' - \sum_j A_{ji} \mu_i$$

and so

$$\boldsymbol{\lambda}'' - A'' \boldsymbol{\mu} = \boldsymbol{\lambda}' - A \boldsymbol{\mu},$$

as desired.

Observe that d is the order of K in $H_1(Y; \mathbb{Z})$. $\square$

Definition 6.4. Let $\boldsymbol{\lambda} \in \bigoplus_{i=1}^{\ell} H_1(T_i^2; \mathbb{Z})$ be a Seifert framing, as constructed above. Then $\boldsymbol{\lambda}^\Sigma$ bounds an oriented surface, F, properly embedded in $Y - N(K)$. We will call any such surface, F, a *(rational) Seifert surface* for the link K. One may also consider contracting $N(K)$ radially to K so that the interior of F is embedded while ∂F is a d-fold cover of K. (Again, d is the order of $[K]$ in $H_1(Y; \mathbb{Z})$.)

Remark 6.5. If Y is not a rational homology sphere, then there may be a $\mathbb{Q}$-linear dependence among the homology classes of the meridians of K in $H_1(Y - N(K); \mathbb{Q})$. Such an occurrence would cause the Seifert framing to be ill-defined. As an example, consider the nullhomologous link $S^1 \times x \cup S^1 \times y$ in $S^1 \times S^2$ for distinct points $x, y \in S^2$. The ambiguity may be resolved by specifying the second homology class of the Seifert surface.

We are now ready to define the Thurston–Bennequin number of a Legendrian link $\mathcal{L}_K$.

Definition 6.6. Let $\mathcal{L}_K$ be a Legendrian representative of a link $K = \bigcup_{i=1}^{\ell} K_i$ of order d in a contact rational homology sphere (Y, ξ), $\boldsymbol{\gamma}$ its contact framing, and $\boldsymbol{\lambda}$ its Seifert framing. Then the *Thurston–Bennequin number* of $\mathcal{L}_K$, $\mathrm{tb}(\mathcal{L}_K) \in \mathbb{Q}$, is

$$\mathrm{tb}(\mathcal{L}_K) = \frac{1}{d}(\boldsymbol{\gamma} \cdot \boldsymbol{\lambda}).$$

As is standard, we use $\boldsymbol{\gamma} \cdot \boldsymbol{\lambda}$ to denote an inner product of algebraic intersection numbers. More precisely,

$$\boldsymbol{\gamma} \cdot \boldsymbol{\lambda} := \sum_{i=1}^{\ell} [\gamma_i] \cdot [\lambda_i],$$

where "$\cdot$" on the right-hand side refers to algebraic intersection number.

Note that an overall reversal of orientations on $\mathcal{L}_K$ will not alter $\mathrm{tb}(\mathcal{L}_K)$. However, changing the orientation of one component of a multi-component link could drastically alter the Seifert framing and thus change the Thurston–Bennequin number.

The following relationship between $\mathrm{tb}(\mathcal{L}_K)$ and $\mathrm{tb}(\mathcal{L}_{\widetilde{K}})$ under a contact cover of degree m is immediate.

Lemma 6.7. *Let $\mathcal{L}_K$ be a Legendrian link in the contact rational homology sphere (Y, ξ) and $\mathcal{L}_{\widetilde{K}}$ its lift to a Legendrian link in an m-fold contact cover $(\widetilde{Y}, \widetilde{\xi})$. Then*

$$\mathrm{tb}(\mathcal{L}_K) = \frac{1}{m} \mathrm{tb}(\mathcal{L}_{\widetilde{K}}).$$

Proof. Note that $\widetilde{Y}$ will also be a rational homology sphere. By construction, $\boldsymbol{\lambda}$ is the image, under the map induced by the projection $\pi \colon \widetilde{Y} \to Y$, of the Seifert framing $\widetilde{\boldsymbol{\lambda}}$ for $\widetilde{K}$. Similarly, $\boldsymbol{\gamma}$ is the image, under π_*, of the contact framing $\widetilde{\boldsymbol{\gamma}}$ for $\widetilde{K}$.

Since

$$\boldsymbol{\gamma} \cdot \boldsymbol{\lambda} = (\pi_* \widetilde{\boldsymbol{\gamma}}) \cdot (\pi_* \widetilde{\boldsymbol{\lambda}}) = \pi_* (\widetilde{\boldsymbol{\gamma}} \cdot \widetilde{\boldsymbol{\lambda}}),$$

we see that

$$\mathrm{tb}(\mathcal{L}_K) = \frac{1}{m} \mathrm{tb}(\mathcal{L}_{\widetilde{K}})$$

as desired. $\qquad\qquad\qquad\qquad\qquad\qquad\qquad\qquad\qquad\qquad\qquad\quad\square$

6.2. Computing $\mathrm{tb}(\mathcal{L}_K)$ from grid diagrams. Since tb behaves simply when taking contact covers (Lemma 6.7), we can compute $\mathrm{tb}(\mathcal{L}_K)$ from combinatorial data on G_K for any grid diagram representing $\mathcal{L}_K$. Recall that G_K represents $\mathcal{L}_K$ if a toroidal front diagram for $\mathcal{L}_K$ can be obtained from G_K by the procedure described in the proof of Theorem 4.4. Since this combinatorial data are most easily expressed in the language of Heegaard Floer homology, we will now mention Heegaard Floer homology to the extent necessary to identify the relevant combinatorial data. See [**BGH08**] for more details.

Associated to a grid number n grid diagram G_K for $K \in L(p, q)$ is a combinatorial Heegaard Floer chain complex, $CF^-(G_K)$, whose generators correspond to one-to-one matchings between the α and β curves. Each generator, $\mathbf{x}$, furthermore comes equipped with a combinatorially defined homological grading, $\mathbf{M}(\mathbf{x}) \in \mathbb{Q}$, as described in Section 2.2.2 of [**BGH08**].

Now let z^- be the generator of $CF^-(G_K)$ in the SW (lower left) corner of the X basepoints and z^+ be the generator of $CF^-(G_K)$ in the NE (upper right) corner of the X basepoints. Abusing notation so that G_K refers to the Legendrian link represented by G_K, we have:

Proposition 6.8.

$$\mathrm{tb}(G_K) = \frac{\mathbf{M}(z^-) + \mathbf{M}(z^+)}{2} - d(p, q, q - 1) - 1$$

Here, $d(p, q, q-1)$ denotes the correction term $d(-L(p, q), q-1)$ as defined inductively in [**OS03**].

Proof. In what follows, let $\widetilde{G}_K$ denote the S^3 grid diagram constructed from G_K as in Lemma 6.1 of [**GRS07**] (see also the discussion following the

statement of Lemma 4.6 in [**BGH08**]), and let $\widetilde{z}^-$ (resp., $\widetilde{z}^+$) denote the preimage of z^- (resp., z^+) in $\widetilde{G}_K$. We combine Theorem 1.1 from [**OST06**] and equation (2) from [**BGH08**] to conclude that

$$
\begin{aligned}
\mathbf{M}(z^-) + \mathbf{M}(z^+) &= \frac{1}{p}\left(\mathbf{M}(\widetilde{z}^-) + \mathbf{M}(\widetilde{z}^+)\right) + 2d(p,q,q-1) + \frac{2(p-1)}{p} \\
&= \frac{2}{p}\left(\mathfrak{tb}(\widetilde{G}_K) + 1 + p \cdot d(p,q,q-1) + (p-1)\right).
\end{aligned}
$$

Lemma 6.7 then implies that

$$
\mathfrak{tb}(G_K) = \frac{\mathfrak{tb}(\widetilde{G}_K)}{p} = \frac{\mathbf{M}(z^-) + \mathbf{M}(z^+)}{2} - d(p,q,q-1) - 1.
$$

$\square$

The classical Thurston–Bennequin invariant is particularly relevant to the Berge conjecture because of the following relationship, a generalization of a result of Matsuda [**Mat06**]. Recall that G_K^* denotes the grid diagram dual to G_K (see Section 2). In particular, if G_K represents a Legendrian link with respect to $(L(p,q), \xi_{\mathrm{UT}})$, then G_K^* corresponds to a Legendrian link with respect to $(L(p,q'), \xi_{\mathrm{UT}})$, where $qq' \equiv -1 \mod p$.

Proposition 6.9.

$$
\mathfrak{tb}(G_K) + \mathfrak{tb}(G_K^*) = -\mathrm{GN}(G_K).
$$

Proof. Let $n = \mathrm{GN}(G_K) = \mathrm{GN}(G_K^*)$. Then G_K and G_K^* lift to grid diagrams for $\widetilde{K} \subset S^3$ and $m(\widetilde{K}) \subset S^3$, respectively, where $m(\widetilde{K})$ denotes the topological mirror of $\widetilde{K}$ in S^3. Both grid diagrams have grid number np. Then, as proved in Section 2 of [**Mat06**] (see also the paragraph following equation (1) of [**Ng06**]), we see that

$$
\mathfrak{tb}(\widetilde{G}_K) + \mathfrak{tb}((\widetilde{G}_K)^*) = -np.
$$

Coupled with Lemma 6.7, this implies that

$$
\mathfrak{tb}(G_K) + \mathfrak{tb}(G_K^*) = -n,
$$

as desired. $\square$

Let $\overline{\mathfrak{tb}}(K)$ denote the maximum $\mathfrak{tb}$ of a Legendrian representative of K. Recalling that if G_K represents $K \subset L(p,q')$, then G_K^* represents $m(K) \subset L(p,q)$ ($qq' \equiv -1 \mod p$), we see that Proposition 6.9 implies:

Corollary 6.10.

$$
\mathrm{GN}(K) \geq -\overline{\mathfrak{tb}}(K) - \overline{\mathfrak{tb}}(m(K))
$$

for each link $K \subset L(p,q')$.

7. Calculations

We conclude with some simple observations about Legendrian realizations of knots in $L(p,q)$ for which some integral surgery yields S^3.

Proposition 7.1. *Let K be a knot in $L(p,q)$ upon which integral surgery yields an integer homology sphere S and $\mathcal{K}$ a Legendrian representative of K with respect to $(L(p,q), \xi_{UT})$. Then*

$$p \cdot \mathrm{tb}(\mathcal{K}) \equiv \pm 1 \mod p.$$

Furthermore, if the corresponding contact surgery coefficient yielding S is k, then $p \cdot \mathrm{tb}(\mathcal{K}) = -kp \pm 1$.

Proof. Let $T^2 = \partial(L(p,q) - \mathcal{K})$ be the torus boundary of a neighborhood of $\mathcal{K}$. We denote by

- $\mu \subset T^2$ an oriented meridian of $\mathcal{K}$ in $L(p,q)$,
- $\gamma \subset T^2$ the contact push-off of $\mathcal{K}$,

Assume that the surgery we perform upon $\mathcal{K} \subset L(p,q)$ to obtain S has coefficient $k \in \mathbb{Z}$ with respect to the contact framing, i.e., if we denote the meridian and standard (*not* necessarily Seifert) longitude of the glued-in solid torus by μ' and λ_0, then

$$\mu' \equiv k\mu + \gamma, \quad \lambda_0 \equiv -\mu.$$

Let $K' := S^1 \times \{0\}$ denote the induced knot in the surgered manifold, S. Since S is an integer homology sphere, $H_1(L(p,q) - N(K)) = H_1(S - N(K')) \cong \mathbb{Z}$, generated by μ', implying that there is a unique $r \in \mathbb{Z}$ such that

$$\lambda' := \lambda_0 + r\mu' = (kr - 1)\mu + r\gamma = 0 \in H_1(L(p,q) - N(K)).$$

Hence, $\mu = r\mu' - \lambda'$.

Since surgery upon K' yields $L(p,q)$, $r = \pm p$. Furthermore, since (μ', λ') form a symplectic basis for $H_1(T^2)$, we have $\mu \cdot \lambda' = r$. The definition of the Seifert framing requires that $\mu \cdot \lambda' = p$. So if $r = -p$, we replace (μ', λ') by $(-\mu', -\lambda')$ (which reverses the orientation on the induced knot, K'). Hence

$$\mu' = \pm(k\mu + \gamma), \quad \lambda' = (kp \mp 1)\mu + p\gamma.$$

Since K has order p in $H_1(L(p,q))$,

$$p \cdot tb(K) = \gamma \cdot \lambda' = -kp \pm 1,$$

as desired. $\square$

Note that if $K \subset L(p,q)$ has an integral surgery yielding S^3, then $K \subset L(p,q')$ (the topological mirror of K) also has an integral surgery yielding S^3. The following is an easy corollary of the preceding proposition:

Corollary 7.2. *If G_K is a diagram of grid number 1 for a Legendrian knot $\mathcal{L}_K \subset (L(p, q'), \xi_{UT})$, $p > 2$, whose underlying topological knot has an integral surgery slope yielding S^3 and G_K^* is the dual* GN1 *diagram representing a Legendrian knot $\mathcal{L}_{K^*}$ in $(L(p, q), \xi_{UT})$, the corresponding contact surgeries on $\mathcal{L}_K$ and $\mathcal{L}_{K^*}$ which yield S^3 are those with surgery coefficients 0 and +1, respectively (or vice versa).*

If $p = 2$, then there is only one Legendrian knot $\mathcal{L}_K$ with a grid number 1 diagram and $G_K = G_K^*$. The 0 and +1 contact surgeries on $\mathcal{L}_K$ are the integral surgeries which yield S^3.

Note that for $p = 1$ there is no grid number 1 diagram of a knot (as defined in this article).

Proof. Assume $p > 2$. By Proposition 6.9,

$$(\star) \qquad\qquad \mathrm{tb}(\mathcal{L}_K) + \mathrm{tb}(\mathcal{L}_{K^*}) = -1.$$

Exchanging the roles of $\mathcal{L}_K$ and $\mathcal{L}_{K^*}$ if necessary, we know, by Proposition 7.1, that

$$\mathrm{tb}(\mathcal{L}_K) = \frac{k_1 p + 1}{p},$$

and

$$\mathrm{tb}(\mathcal{L}_{K^*}) = \frac{k_2 p - 1}{p},$$

where $k_1, k_2 \in \mathbb{Z}$. By equation $(\star)$, $k_1 + k_2 = -1$.

Since any Stein filling of S^3 is diffeomorphic to B^4 [**Eli90**], $(L(p, q), \xi_{UT})$ is Stein fillable for all $L(p, q)$ [**Hon00**], and any negative contact surgery can be turned into a sequence of -1 contact surgeries [**DG04**], we can conclude that $k_1, k_2 \leq 0$, since positive k_i would yield a negative contact surgery coefficient by Proposition 7.1, leading to a non-standard Stein filling of S^3.

Therefore, $k_1 + k_2 = -1$ implies that $k_1 = 0$ and $k_2 = -1$, or vice versa. In other words, contact 0 surgery on one of the two Legendrian knots and contact $+1$ surgery on the other yields S^3.

Now assume $p = 2$. One readily observes that there is a single knot K with a grid number 1 diagram G_K and this diagram equals its dual. The associated Legendrian knot $\mathcal{L}_K$ admits a toroidal front diagram with no cusps or crossings, hence it is a simple closed curve on the Heegaard torus and the contact framing is the surface framing. Since the knot crosses each α and β just once, contact 0 surgery yields S^3. The contact $+1$ surgery may be viewed as effecting a Dehn twist upon α along K with the result crossing β only once, hence producing S^3.

Any other integral surgery K cannot create S^3. Other than the meridian μ of K, there is a single curve λ on $\partial N(K)$ that intersects both the 0 and $+1$ contact surgery slopes once. The exterior of K is a solid torus and λ is

its meridian. The slope of a surgery creating S^3 necessarily intersects λ just once. The only slopes that also intersect μ once are the 0 and +1 contact slopes. $\square$

Acknowledgments

References

[Ber]   J. Berge, *Some knots with surgeries yielding lens spaces*, unpublished manuscript.

[BGH08]   K.L. Baker, J.E. Grigsby and M. Hedden, *Grid diagrams for lens spaces and combinatorial knot Floer homology*, Internat. Math. Res. Notices (2008), article ID rnn024, 39 pp., doi:10.1093/imrn/rnn024.

[BL89]   S.A. Bleiler and R.A. Litherland, *Lens spaces and Dehn surgery*, Proc. Amer. Math. Soc. **107**(4) (1989), 1127–1131.

[BR77]   J. Bailey and D. Rolfsen, *An unexpected surgery construction of a lens space*, Pacific J. Math. **71**(2) (1977), 295–298.

[Bru98]   H. Brunn, *Uber verknotete kurven*, Verhandlugen des ersten Internationalen Mathematiker-Kongresses, Zurich, 1898, 256–259.

[Cro95]   P.R. Cromwell, *Embedding knots and links in an open book. I. Basic properties*, Topol. Appl. **64**(1) (1995), 37–58.

[DG04]   F. Ding and H. Geiges, *A Legendrian surgery presentation of contact 3-manifolds*, Math. Proc. Cambridge Philos. Soc. **136**(3) (2004), 583–598.

[Dyn06]   I.A. Dynnikov, *Arc-presentations of links: monotonic simplification*, Fund. Math. **190** (2006), 29–76.

[Eli90]   Y. Eliashberg, *Filling by holomorphic discs and its applications*, in 'Geometry of low-dimensional manifolds, 2 (Durham, 1989)', **151**, 45–67, London Math. Soc. Lecture Note Ser., Cambridge Univ. Press, Cambridge, 1990.

[FS80]   R. Fintushel and R. J. Stern, *Constructing lens spaces by surgery on knots*, Math. Z. **175**(1) (1980), 33–51.

[FT97]   D. Fuchs and S. Tabachnikov, *Invariants of Legendrian and transverse knots in the standard contact space*, Topology **36**(5) (1997), 1025–1053.

[Gab87]   D. Gabai, *Foliations and the topology of 3-manifolds. III*, J. Differential Geom. **26**(3) (1987), 479–536.

[Gei06]   H. Geiges, *Contact geometry*, in Handbook of differential geometry, **II**, Elsevier/North-Holland, Amsterdam, 2006, 315–382.

[GL89]   C.McA. Gordon and J. Luecke, *Knots are determined by their complements*,
           J. Amer. Math. Soc. **2**(2) (1989), 371–415.

[GRS07]   J.E. Grigsby, D. Ruberman and S. Strle, *Knot concordance and Heegaard Floer
           homology invariants in branched covers*, Geom. Top. 12(4) (2008), 2249–2275,
           math.GT/0701460.

[Hon00]   K. Honda, *On the classification of tight contact structures I*, Geom. Topol. **4**
           (2000), 309–368 (electronic).

[Lyo80]   H.C. Lyon, *Torus knots in the complements of links and surfaces*, Michigan
           Math. J. **27**(1) (1980), 39–46.

[Mat06]   H. Matsuda, *Links in an open book decomposition and in the standard contact
           structure*, Proc. Amer. Math. Soc. **134**(12) (2006), 3697–3702 (electronic).

[MM07]   H. Matsuda and W.W. Menasco, *On rectangular diagrams, Legendrian knots
           and transverse knots*, math.GT/0708.2406, 2007.

[Mos71]   L. Moser, *Elementary surgery along a torus knot*, Pacific J. Math. **38** (1971),
           737–745.

[MOS06]   C. Manolescu, P. Ozsváth and S. Sarkar, *A combinatorial description of knot
           Floer homology*, math.GT/0607691, 2006.

[MOST06]   C. Manolescu, P. Ozsváth, Z. Szabó and D. Thurston, *On combinatorial link
           Floer homology*, math.GT/0610559, 2006.

[Ng06]   L. Ng, *On arc index and maximal Thurston-Bennequin number*,
           math.GT/0612356, 2006.

[NOT07]   L. Ng, P. Ozsváth, and D. Thurston, *Transverse knots distinguished by knot
           Floer homology*, math.GT/0703446, 2007.

[OS03]   P. Ozsváth and Z. Szabó, *Absolutely graded Floer homologies and intersection
           forms for four-manifolds with boundary*, Adv. Math. **173**(2) (2003), 179–261.

[OS05]   P. Ozsváth and Z. Szabó, *Heegaard Floer homology and contact structures*,
           Duke Math. J. **129**(1) (2005), 39–61.

[OST06]   P. Ozsváth, Z. Szabó and D. Thurston, *Legendrian knots, transverse knots and
           combinatorial Floer homology*, math.GT/0611841, 2006.

[Özt05]   F. Öztürk, *Generalized Thurston-Bennequin invariants for real algebraic sur-
           face singularities*, Manuscripta Math. **117**(3) (2005), 273–298.

[Świ92]   J. Świątkowski, *On the isotopy of Legendrian knots*, Ann. Global Anal. Geom.
           10(3) (1992), 195–207.

Department of Mathematics
University of Miami
PO Box 249085
Coral Gables, FL 33124-4250
E-mail address: k.baker@math.miami.edu

Department of Mathematics
Columbia University
2990 Broadway; MC4406
New York, NY 10027
E-mail address: egrigsby@math.columbia.edu